Microscopic origin of *n*-type behavior in Si-doped AlN

Daniel Fernández Hevia* and Catherine Stampfl
School of Physics, The University of Sydney, Sydney 2006, NSW Australia

Francesc Viñes and Francesc Illas
Departament de Quimica Fisica and Institut de Quimica Teórica i Computacional (IQTCUB), Universitat de Barcelona, C/ Marti i Franqués 1, E-08028 Barcelona, Spain

(Received 23 June 2012; revised manuscript received 9 July 2013; published 8 August 2013)

In contrast to a long held belief, it has been shown that *n*-type AlN can be achieved through Si-doping. This is unexplainable from the current theoretical understanding, a situation that hinders further progress in AlN-based ultraviolet (UV) technologies. From first-principles calculations, we find that *n*-type behavior arises under N-rich growth conditions due to high Si solubility and to the formation of V_{Al}-bound Si clusters. We show that metal-rich growth may lead to weak *n*-type behavior due to oxygen impurities binding and deactivating cation vacancies. We provide clues for designing production processes for *n*-type AlN as a base material for potential new UV sources.

DOI: 10.1103/PhysRevB.88.085202 PACS number(s): 31.15.A−, 71.20.−b, 41.85.−p, 72.20.−i

I. INTRODUCTION

Due to its very wide band gap (∼6.2 eV),[1] AlN has significant potential applications in ultraviolet UV and deep-UV sources and detectors through *n*-type doping.[2] Achieving efficient and controllable doping in AlN is a challenge, since AlN is widely perceived as an insulator. Recent success in *n*-type doping with silicon[3–6] has led to an upsurge of experimental activity in the field. Despite the experimental results, the microscopic doping mechanism is not known. This mechanism is a key factor that needs to be understood in order to promote development of AlN-based devices. Recently some publications[7,8] have investigated fundamental properties of Si-doping in AlN. The results indicate a shallow donor character for this dopant, instead of the *DX*-states predicted before.[9,10] Previous theoretical investigations of semiconductor AlN addressed the stability of vacancies and impurities.[11–14] These studies pointed out that the formation energy of the $\mathrm{Si_{Al}}$ donor is not low enough to overcome the native V_{Al} compensating acceptor. Nevertheless, *n*-type conductivity has been experimentally detected for Si-doped wurtzite-AlN,[3–6] although with remarkable differences which, in principle, depend on the growth techniques. For example, growth by plasma assisted molecular beam epitaxy (PAMBE) on 6H-SiC[5,6] or sapphire[15] under N-rich conditions shows high electron density ($\sim 8\times10^{17}$) and low mobility (∼8 $\mathrm{cm^2\ V^{-1}\ s^{-1}}$). Conversely, semi-insulating behavior has been found under Al-rich conditions.[15] For Si-doped AlN grown by metal-organic chemical vapor deposition (MOCVD) on sapphire,[3] lower electron densities $\sim10^{17}$ and mobilities ∼2 $\mathrm{cm^2\ V^{-1}\ s^{-1}}$ have been achieved, while low electron density ($\sim10^{15}$) and high mobility (125 $\mathrm{cm^2\ V^{-1}\ s^{-1}}$) were reported for Si-doped AlN grown by metal-organic vapor phase epitaxy (MOVPE) on $\mathrm{Al_2O_3}$[16] or 4H-SiC substrates.[4] All in all, the origin and the relation to preparation conditions of *n*-type behavior (and its associated *n*-type conductivity) in Si-doped AlN remains unclear and a matter of debate. In this paper we perform density functional theory[17] total-energy calculations using the local-density approximation,[18] for both the wurtzite (wz) and zincblende (zb) phases, in order to predict the species responsible for the observed *n*-type behavior, and to rationalize the dependence of this behavior on preparation conditions.

II. METHODOLOGY

We use first-principles norm-conserving pseudopotentials[20] that were thoroughly tested in earlier work.[19] We adopt the supercell approach, using the $4a \times 4b \times 3c$–192 atom wz supercell for all our calculations. For the zb phase we use a 216-atom supercell, being $3 \times 3 \times 3$ the conventional 8-atom fcc cell. We study both the maximum-symmetry configurations as well as broken-symmetry structures. The whole supercells are fully relaxed to less than 3 meV/a.u. forces on the atoms. We use a 50-Ry cutoff energy and a Brillouin-zone sampling consisting of one special **k** point (shifted from the **Γ** point).[21] Extensive tests (plots of formation energies of all relevant defects vs cutoff energy and supercell size) show that we obtain well converged formation energies within ±40 meV. The formation energy of a certain defect X in charge state q is[22] $\Delta H_f(X^q; E_F) = E_{\mathrm{tot}}(X^q) - E_{\mathrm{tot}}^{(\mathrm{bulk})} - \sum_{i=1}^{k} n_i\mu_i + q(E_F + E_V^c)$, where $E_{\mathrm{tot}}(X^q)$ is the total energy of the defect supercell and $E_{\mathrm{tot}}^{(\mathrm{bulk})}$ is that of the ideal defect-free supercell. The index i labels the atom species in the system, n_i is the number of atoms of type i added or removed to create the defect, and μ_i is the corresponding chemical potential. E_{F} is the Fermi level referenced to the bulk valence band maximum (VBM). The range for E_{F} is taken to be the value of the band gap (as per a *GW* calculation).[23] $E_V^c = E_V + \Delta V$ is the VBM, E_V, corrected by an energy shift that aligns the reference potential in the supercell-with-defect calculation with that in the pure-bulk calculation.[24] For defect complexes, the binding energy is defined (for the simple case of a two-constituent complex $X \equiv AB$) as $E_b(X^{q_X}) = \Delta H_f(A^{q_A}) + \Delta H_f(B^{q_B}) - \Delta H_f(X^{q_X})$, where $q_X = q_A + q_B$. All μ_i are calculated from first principles within the same formalism.

Regarding the host and impurity atoms chemical potentials, physical growth conditions impose certain bounds.

Note that

$$\mu_{\mathrm{Al(AlN)}} + \mu_{\mathrm{N(AlN)}} = \mu_{\mathrm{AlN(bulk)}} = \mu_{\mathrm{Al(bulk)}} + \mu_{\mathrm{N(bulk)}} + \Delta H_f(\mathrm{AlN}), \quad (1)$$

where $\Delta H_f(\mathrm{AlN})$ is the heat of formation of aluminum nitride, and the notation $\mu_{\mathrm{Al(AlN)}}$ indicates the chemical potentials of Al atoms when residing in the bulk AlN material, while $\mu_{\mathrm{Al(bulk)}}$ indicates the chemical potentials of Al atoms when residing in bulk aluminum. In the case of nitrogen, $\mu_{\mathrm{N(bulk)}} \equiv \mu_{\mathrm{N_2}}$ must be understood as the chemical potential of N atoms when in the stable gaseous N_2 phase. The quantities $\mu_{\mathrm{Al(AlN)}}$ and $\mu_{\mathrm{N(AlN)}}$ are the variables, while $\mu_{\mathrm{Al(bulk)}}$, $\mu_{\mathrm{N(bulk)}}$, and $\mu_{\mathrm{AlN(bulk)}}$, are constants that can be calculated from first principles as total energies. Next we note that

$$\mu_{\mathrm{Al(AlN)}} \leqslant \mu_{\mathrm{Al(bulk)}}, \quad (2)$$

i.e., the chemical potential of Al in AlN can not be greater than the chemical potential in bulk Al, otherwise Al atoms would form bulk Al droplets instead of incorporating to the growing AlN crystal. Now, according to

$$\mu_{\mathrm{Al(AlN)}} + \mu_{\mathrm{N(AlN)}} = \mu_{\mathrm{AlN(bulk)}} \equiv \text{const.}, \quad (3)$$

the maximum allowed value of $\mu_{\mathrm{Al(AlN)}}$ will correspond to the minimum allowed value of $\mu_{\mathrm{N(AlN)}}$, i.e.: when $\mu_{\mathrm{Al(AlN)}} = \mu^{\mathrm{max}}_{\mathrm{Al(AlN)}} = \mu_{\mathrm{Al(bulk)}}$, then $\mu_{\mathrm{N(AlN)}}$ must be $\mu^{\mathrm{min}}_{\mathrm{N(AlN)}}$ given by

$$\mu^{\mathrm{min}}_{\mathrm{N(AlN)}} = \mu_{\mathrm{AlN(bulk)}} - \mu_{\mathrm{Al(bulk)}} = \mu_{\mathrm{N(bulk)}} + \Delta H_f(\mathrm{AlN}),$$

where we have used Eq. (1).

Exactly the same argument shows that

$$\mu^{\mathrm{min}}_{\mathrm{Al(AlN)}} = \mu_{\mathrm{AlN(bulk)}} - \mu^{\mathrm{max}}_{\mathrm{N(AlN)}} = \mu_{\mathrm{AlN(bulk)}} - \mu_{\mathrm{N(bulk)}},$$

which, again by using Eq. (1), yields

$$\mu^{\mathrm{min}}_{\mathrm{Al(AlN)}} = \mu_{\mathrm{Al(bulk)}} + \Delta H_f(\mathrm{AlN}).$$

Therefore, the limits for the chemical potentials are as follows: For aluminum, $\mu_{\mathrm{Al(bulk)}} + \Delta H_f(\mathrm{AlN}) \leqslant \mu_{\mathrm{Al(AlN)}} \leqslant \mu_{\mathrm{Al(bulk)}}$. The Al-poor (or N-rich) limit corresponds to $\mu_{\mathrm{Al(AlN)}} = \mu_{\mathrm{Al(bulk)}} + \Delta H_f(\mathrm{AlN})$. The Al-rich (or N-poor) limit, where a little bit more aluminum would lead to the formation of Al-bulk droplets instead of an Al-enriching of the AlN material, corresponds to $\mu_{\mathrm{Al(AlN)}} = \mu_{\mathrm{Al(bulk)}}$. For nitrogen $\mu_{\mathrm{N(bulk)}} + \Delta H_f(\mathrm{AlN}) \leqslant \mu_{\mathrm{N(AlN)}} \leqslant \mu_{\mathrm{N(bulk)}}$. Now the N-poor (or Al-rich) limit corresponds to the case $\mu_{\mathrm{N(AlN)}} = \mu_{\mathrm{N(bulk)}} + \Delta H_f(\mathrm{AlN})$, while the N-rich (or Al-poor) limit (where N_2 molecules are about to form) corresponds to $\mu_{\mathrm{N(AlN)}} = \mu_{\mathrm{N(bulk)}}$. In summary:

$$\underset{\text{(Al-poor/N-rich limit)}}{\mu_{\mathrm{AlN(bulk)}} - \mu_{\mathrm{N(bulk)}}} \leqslant \mu_{\mathrm{Al(AlN)}} \leqslant \underset{\text{(N-poor/Al-rich limit)}}{\mu_{\mathrm{Al(bulk)}}} \quad (4)$$

and

$$\underset{\text{(N-poor/Al-rich limit)}}{\mu_{\mathrm{AlN(bulk)}} - \mu_{\mathrm{Al(bulk)}}} \leqslant \mu_{\mathrm{N(AlN)}} \leqslant \underset{\text{(Al-poor/N-rich limit)}}{\mu_{\mathrm{N(bulk)}}}. \quad (5)$$

Note that the higher (the less negative) is the chemical potential of any constituent, the more rich is the system in that constituent. In order to establish the same kind of limits for the impurities/dopants, we note that the impurities are not constrained by an equation such as Eq. (3): there is no lower limit for its chemical potential. What one can find is an upper bound, which, in fact, is the limit that defines the solubility of the defect.

In the case of oxygen in AlN, this limit is defined by the formation of sapphire, Al_2O_3, through the limiting equation:

$$\forall \mu_{\mathrm{Al(AlN)}}: \quad 2\mu_{\mathrm{Al(AlN)}} + 3\mu^{\mathrm{max}}_{\mathrm{O(AlN)}} = \mu_{\mathrm{Al_2O_3(bulk)}}. \quad (6)$$

What Eq. (6) means is that, for a given value of $\mu_{\mathrm{Al(AlN)}}$, the maximum chemical potential that the oxygen atoms can attain is that one that would make exactly as possible to have the O atoms incorporated to the AlN host, as to have the O atoms forming a secondary Al_2O_3 phase in the growth chamber. Hence, the maximum value for the oxygen chemical potential as an impurity in AlN, $\mu^{\mathrm{max}}_{\mathrm{O(AlN)}}$, depends on the actual value of the Al-chemical potential. For each value of $\mu_{\mathrm{Al(AlN)}}$, we have

$$\mu^{\mathrm{max}}_{\mathrm{O(AlN)}} = \tfrac{1}{3}\mu_{\mathrm{Al_2O_3(bulk)}} - \tfrac{2}{3}\mu_{\mathrm{Al(AlN)}}. \quad (7)$$

Given that $\mu_{\mathrm{Al_2O_3(bulk)}}$ is a constant, Eq. (7) represents a straight line for $\mu^{\mathrm{max}}_{\mathrm{O(AlN)}}$ as a function of $\mu_{\mathrm{Al(AlN)}}$. Therefore, as we said, we have a different value of $\mu^{\mathrm{max}}_{\mathrm{O(AlN)}}$ for each allowed value of $\mu_{\mathrm{Al(AlN)}}$.

For silicon, calculations by Li and Brenner[25] indicate that the gas-phase growth atmosphere is undersaturated with respect to nitrogen, making it more easy to form Si islands than to grow Si_3N_4 species. In fact, in the PAMBE studies where high n-type conductivity was achieved (under N-rich conditions), there is evidence pointing to crystalline silicon as the solubility-limiting phase (SLP), hence providing a high chemical potential for Si in AlN. This is also in agreement with its observed large solubility (homogeneous incorporation in excess of 5×10^{21} cm^{-3}).[26] It is worth mentioning that a previous theoretical study used crystalline silicon as the SLP of Si_{Al},[13] although neither the V_{Al} nor the microscopic doping mechanism were addressed.

Therefore the solubility limit of silicon in AlN is defined by the formation of crystalline silicon through the limiting equation:

$$\forall \mu_{\mathrm{N(AlN)}}: 4\mu_{\mathrm{N(AlN)}} + 3\mu^{\mathrm{max}}_{\mathrm{Si(AlN)}} = \mu_{\mathrm{Si(bulk)}}. \quad (8)$$

Now, what Eq. (8) means is that the maximum value for the silicon chemical potential as an impurity in AlN, $\mu^{\mathrm{max}}_{\mathrm{Si(AlN)}}$, depends on the actual value of the N-chemical potential. For each value of $\mu_{\mathrm{N(AlN)}}$, we have

$$\mu^{\mathrm{max}}_{\mathrm{Si(AlN)}} = \tfrac{1}{3}\mu_{\mathrm{Si(bulk)}} - \tfrac{4}{3}\mu_{\mathrm{N(AlN)}}. \quad (9)$$

Again, given that μ_{Si} is a constant, Eq. (9) represents a straight line for $\mu^{\mathrm{max}}_{\mathrm{Si(AlN)}}$ as a function of $\mu_{\mathrm{N(AlN)}}$.

In summary, chemical potentials for Al and N have been assumed to be limited by the formation of bulk Al and N_2 respectively, while silicon and oxygen solubilities were assumed to be limited by formation of Si, and sapphire Al_2O_3 respectively. All the chemical potentials were calculated from first principles within the same formalism, and compare well with both experimental values and other first-principles calculations.

III. RESULTS AND DISCUSSION

We study the energetics, atomic geometry, and electronic structure of nV_{Al}, nV_{N} $(1 \leqslant n \leqslant 4)$, Al_i, $\mathrm{Al_N}$, $\mathrm{N_{Al}}$, $(\mathrm{N_2})_{\mathrm{N}}$,

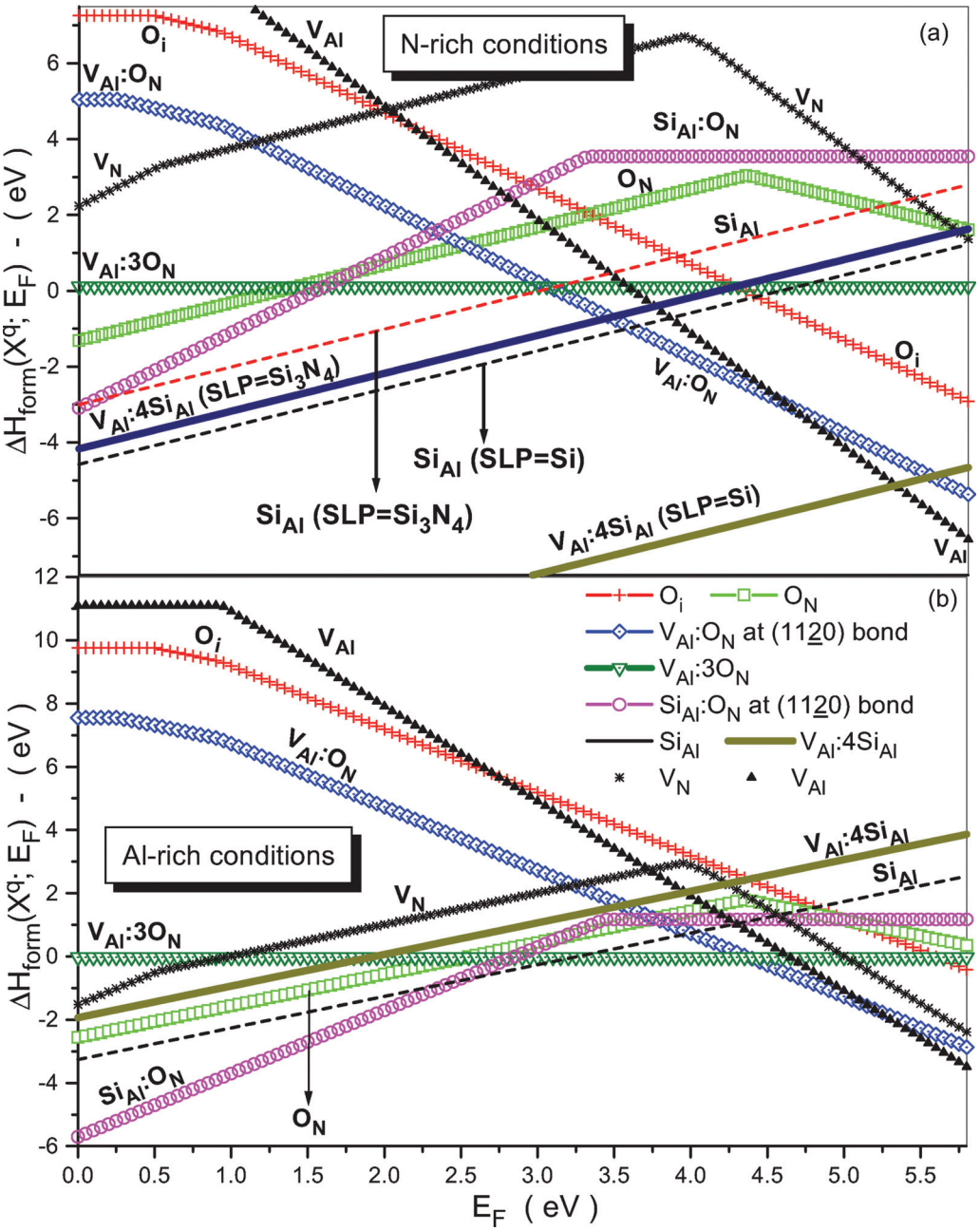

FIG. 1. (Color online) Formation energy of relevant defects as a function of the Fermi level position within the band gap. (a) N-rich (showing results for both crystalline Si and Si_3N_4 as solubility limiting phases); (b) Al-rich (using Si_3N_4 as SLP). All defects are shown in all stable charge states (changes of slope mark the thermodynamic transition levels).

$(N_2)_{Al}$, V_{Al}:V_N, nO_N ($n = 1$ and 6), mSi_{Al}, and V_{Al}:mSi_{Al} with $1 \leqslant m \leqslant 6$, $2V_{Al}$:$6Si_{Al}$, Si_{Al}:O_N, O_i, $(O_2)_N$, V_{Al}:nO_N ($n = 1$, 3, and 6), Si_{Al}:nV_N ($1 \leqslant n \leqslant 4$), O_N:nV_N ($1 \leqslant n \leqslant 3$), and Al_i:Si_{Al}. Interstitials are considered in octahedral, tetrahedral, split, and hexagonal geometries. We always find that the octahedral site is the lowest-energy configuration. All defect pairs are considered as nearest neighbor (nn) along the *c* axis, or transverse to it. We always find the transverse geometry around 0.4 eV lower in energy. For the V_{Al}:$3O_N$ system, we consider three possible geometries, the most favorable being that where the three O atoms occupy the three equivalent basal-plane N sites nn to the V_{Al}. For the mSi_{Al} clusters and the V_{Al}:mSi_{Al} complexes (with $1 \leqslant m \leqslant 6$), we consider a large number of different geometries, the most favorable being those where the Si_{Al} atoms and the V_{Al} lie in the same basal plane.

In Fig. 1 we present the formation energies of the relevant defects in Si-doped wz-AlN, in all stable charge states, for both N- and Al-rich conditions. A first inspection of the results reveals that Si clustering is, in itself, not favorable (see N-rich conditions below), with binding energies becoming more and more negative upon adding Si atoms to the cluster [note that $E_b(X^{qx})$ is defined such that binding corresponds to positive energies]. However, clustering is strongly promoted by charged cation vacancies that electrostatically stabilize the

Si aggregates, allowing the formation of very strong Si-N and N-N covalent bonds. For any n and for any charge state, the ΔH_f of V_{Al}:nSi$_{Al}$ is always much lower than that of the corresponding nSi$_{Al}$. There are stable, high-charge states for the nSi$_{Al}$ complexes that do not exist for the V_{Al}:nSi$_{Al}$ systems: e.g., the 6+ charge state of the planar hexagonal ringlike geometry of the 6Si$_{Al}$ complex, which is very stable under strongly p-type conditions.

Figure 1 shows furthermore that oxygen is a negative-U defect, undergoing a shallow-to-deep DX-like structural transition. This agrees with previous calculations[7,8,11] and with recent experimental results from electron paramagnetic resonance and electron-nuclear double resonance.[27] Other defects also exhibit negative-U behavior: unstable charge states and thermodynamic transition levels involving transfer of more than one electron. For example, V_{Al} changes from the neutral charge state to the 3- state (with the 1- and 2- states being unstable), while V_N behaves as an amphoteric defect changing from donor to acceptor without a stable neutral state. This kind of charge-dependent stability is characteristic of negative-U defects. We find that Si$_{Al}$ causes only small lattice distortions, without any DX-like transition.

Focusing on the V_{Al}:4Si$_{Al}$ and V_{Al}:3O$_N$ complexes, we have analyzed in detail their atomic and electronic structures (see Figs. 2 and 3). For the former, the lowest energy structure is always the one that minimizes the perturbation of the p_z-like lone pair of the V_{Al} c-axis nn N-atom. The system encourages planar geometries where the nitrogen lone pair remains almost unaffected, and becomes the highest fully occupied gap state. The three singlet gap states are occupied for the V$_{Al}$:4Si$_{Al}$ cluster, the upper level being again the p_z-like nitrogen lone pair lying right below the cation vacancy. Figure 3 shows a sketch of the gap state levels. We shall now discuss, in the light of our results, the experimentally observed n-type conductivity and its dependence on growth conditions.

A. N-rich conditions

The most likely Si-accommodating defect is a V$_{Al}$:4Si$_{Al}$ complex. Experiments reporting growth under N-rich conditions correspond to MBE techniques[5,6,15] and report that the solubility limit is defined by crystalline-Si formation.[15,26,28] Our results predict that Si-doped AlN, grown under N-rich conditions, shows n-type doping: the V$_{Al}$:4Si$_{Al}$ complex is a favorable shallow donor with high solubility (due to low formation energy); hence, a high electron density is expected, directly correlated with this high solubility. The large size of the cluster is consistent with the observed low mobility, which we predict to be anisotropic due to the planar nature of the complex. We note that experiments on Si-doped AlN grown by MOCVD,[3] result in a similar electron density and mobility as those by MBE. Although it is commonly assumed that gas phase techniques such as MOCVD or MOVPE work on Al-rich conditions (due to the large binding energy of the N_2 molecule), recent theoretical calculations[25] show that this may not be the case: N_2 is actually proven to be undersaturated with respect to the crystal. For such a case, the N-containing growth precursors are Al$_n$N species, making it possible to attain N-rich conditions for MOCVD growth. Our calculations

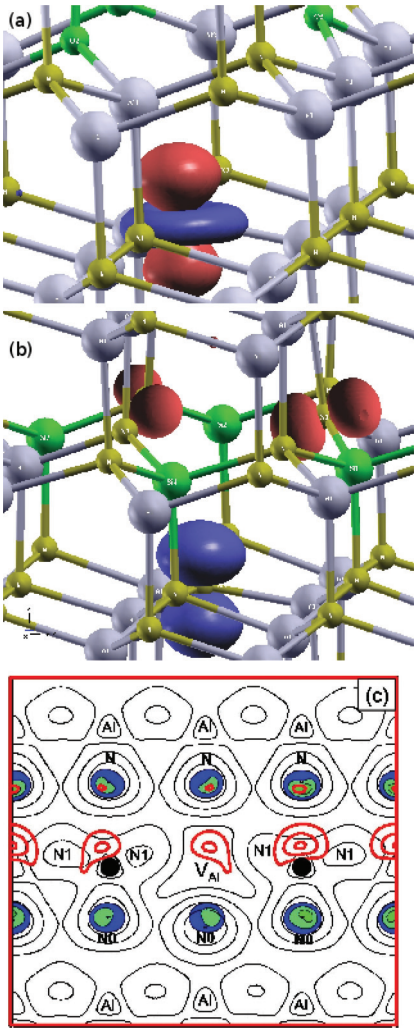

FIG. 2. (Color online) (a) Relaxed geometry and D1 (blue) and S1 (red) defect electronic states for the V$_{Al}$:3O$_N$ complex; green, yellow, and gray spheres denote O, N, and Al atoms, respectively. (b) Relaxed geometry and S1-S3 gap states for the V$_{Al}$:4Si$_{Al}$ cluster; here, green spheres denote Si atoms. (c) Total charge density of the V$_{Al}$:4Si$_{Al}$ cluster in a $(10\bar{1}0)$-plane containing two Si atoms, represented as big black dots. Superimposed to it we show the CB-edge state (s-like N-centered charge densities), and the S0 singlet (shown as thick red lines close to the Si atoms). Energy level notation is in Fig. 3.

show that n-type conductivity exhibited by MOCVD-grown samples (e.g., Ref. 3) is consistent with N-rich growth.

The lowest-energy O-accommodating defect, for E_F in the upper part of the gap, is the $(V_{Al}:O_N)^{2-}$ pair. The pair binding energy in the 2- charge state is 2.5 eV. However, in the n-type limit, oxygen may also enter as octahedral interstitial (see the O_i formation energies in Fig. 1), in agreement with electron energy loss spectroscopy.[29] Oxygen, therefore, acts as a quite stable electron acceptor under n-type N-rich conditions, according to the low formation energies of both the interstitial and the $(V_{Al}:O_N)^{2-}$ pair in the n-type limit (right side of the figures, Fermi level closest to the conduction band) in part (a) of Fig. 1. Acting as an acceptor, oxygen enhances electron-killing effects and its presence is harmful for achieving n-type material. Note that, under these conditions, the isolated substitutional O_N is much higher in energy. This scenario is

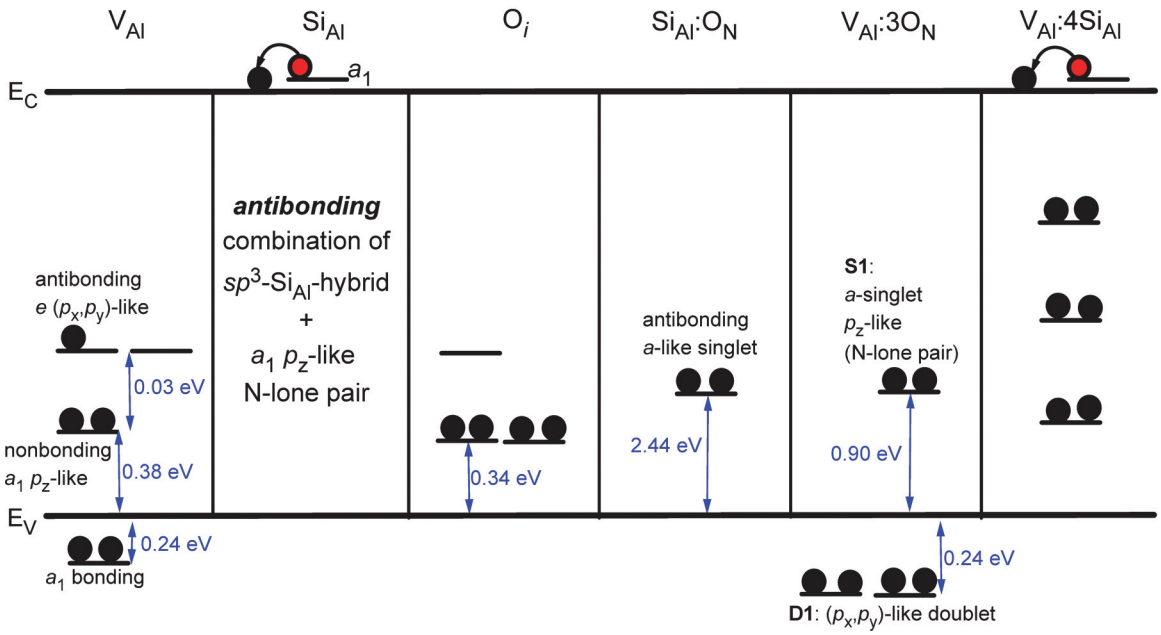

FIG. 3. (Color online) Scheme of Kohn-Sham eigenvalues.

very similar for both the wz and the zb phases, although in the zb phase, O_N does not undergo a *DX* transition nor lead to an improved dopability of the cubic structure, since isolated O_N is not the main relevant defect for *n*-type material.

In summary, Si becomes an efficient *n*-type dopant by clustering around cation vacancies. The formation energy of one particular $(V_{Al}{:}4Si_{Al})^{1+}$ defect complex is much lower than that of the isolated Si_{Al}^{1+}, which provides a Si-based donor able to overcome the V_{Al} acceptor. Clustering is shown to occur only under N-rich growth conditions, and to be depend on the solubility limiting phase, revealing a significant stimulation for those growth techniques and conditions pointing towards the SLP being the formation of a crystalline Si phase.

B. Al-rich conditions

AlN samples grown under Al-rich conditions are mostly semi-insulating.[15,30] This is understandable in view of the results in Fig. 1. In particular, Fig. 1(b) shows that formation of the $V_{Al}{:}4Si_{Al}$ complex is inhibited, leaving no efficient way for achieving *n*-type doping.

Perplexingly, however, under Al-rich conditions, low electron densities (i.e., small *n*-type conductivity in the MOVPE results of Refs. 4 and 16) and a conductivity enhancement with increasing O content (in the MOCVD-grown samples of Ref. 31) have been reported. In order to understand the rationale behind these seemingly contradictory results, we will analyze the Si- and O-accommodating defects in more detail, and their relationship with an insulating or *n*-type behavior.

We first note that the two main Si-accommodating defects (under Al-rich conditions) are the vacancy-substitutional complex and the isolated substitutional (see the $Si_{Al}{:}O_N$ and the Si_{Al} lines in Fig. 1). Of these two Si-accommodating options, the vacancy-substitutional complex is a negative-*U* defect that exists in a stable, donor-like, $(Si_{Al}{:}O_N)^{2+}$ configuration but becomes unstable upon capturing one electron, relaxing (through a *DX*-like structural transition) to a deep, neutral, low-symmetry, strongly lattice-coupled state. This occurs both in the zb and the wz phases. When the Fermi level is above mid-gap (i.e., for moderate *n*-type conditions) the isolated substitutional, Si_{Al}, is the only favorable donor, although it is incapable (in view of its higher formation energy) of overcoming the abundance of electron-killing cation vacancies.

However, the key result here is that when the Fermi level is above mid-gap (i.e., for moderate *n*-type conditions), the O-accommodating defect is the neutralizing $V_{Al}{:}3O_N$ complex, with a large binding energy of 6.3 eV (or 2.1 eV/O-atom). This O-accommodating defect deactivates the electron-acceptor isolated cation vacancies by incorporating them to the complex. The $V_{Al}{:}3O_N$ complex plays a gettering role for the cation vacancies. This is similar to the recently studied role of donor-impurity complexes in As- or Sb-doped silicon:[32,33] $V_{Si}{:}3As_{Si}$ complexes are found to deactivate As in Si. Therefore, under Al-rich conditions, moderately *n*-type material can indeed be achieved by incorporating oxygen and forming the $V_{Al}{:}3O_N$ complex, hence explaining the unexpected increase of conductivity with oxygen content reported in Ref. 31. Within a narrow range above mid-gap, Si_{Al} becomes an active Si-related donor, not compensated by the V_{Al}, which has been gettered and deactivated by the prevalent oxygen-accommodating complex. This situation is possibly responsible for the weakly *n*-type samples, with low free-carrier densities,[4,16] but with potentially good transport properties due to the pointlike nature of the doping defect. Therefore, it is understandable that metal rich growth leads to semi-insulating or weakly *n*-type behavior, depending on the growth technique: The key is the oxygen accommodating defect, which our calculations indicate that could be the neutral $V_{Al}{:}3O_N$ complex, which deactivates the native compensating V_{Al} defect.

IV. CONCLUSIONS

In conclusion, we have studied the mechanism of *n*-type doping in Si-doped AlN, its dependence on growth conditions, and the controversial role of oxygen. We found that efficient doping results from the formation of covalent Si clusters, electrostatically stabilized by cation vacancies. This mechanism is active under N-rich conditions. Oxygen contamination is undesirable in this case because it leads to compensating defects. We have also found that weak *n*-type behavior may be possible under Al-rich conditions, but in this case, conversely, due to an oxygen-accommodating defect that deactivates the compensating V_{Al}. Thus, oxygen contamination may be desirable in this latter case. The present results help to rationalize the efficient and controllable Si doping, as well as the reported differences in achieved carrier densities and mobilities, unraveling the origin of the conflicting experimental reports on the role of oxygen and silicone. This proposed microscopic understanding opens a range of feasible options for potentially efficient UV technologies based on *n*-doped Si:AlN.

ACKNOWLEDGMENTS

Authors D.F.H. and F.I. acknowledge support from Spanish MICINN/MINECO Grants IPT-120000-2010-31 and IPT-120000-2010-19. F.V. thanks the Spanish MICINN for the postdoctoral grant under the program Juan de la Cierva (JCI-2010-06372).

*Current address: Chemistry Departament, University of Las Palmas de Gran Canaria, Campus Universitario de Tafira, 35017 Las Palmas de Gran Canaria and INAEL Electrical Systems, Jarama 5, 45007 Toledo, Spain; dfernandez@proyinves.ulpgc.es, dfhevia@inael.com

[1] N. Nepal, K. B. Nam, M. L. Nakarmi, J. Y. Lin, H. X. Jiang, J. M. Zavada, and R. G. Wilson, Appl. Phys. Lett. **84**, 1090 (2004).
[2] Y. Taniyasu, M. Kasu, and T. Makimoto, Nature (London) **441**, 325 (2006).
[3] M. L. Nakarmi, K. H. Kim, K. Zhu, J. Y. Lin, and H. X. Jiang, Appl. Phys. Lett. **85**, 3769 (2004).
[4] Y. Taniyasu, M. Kasu, and T. Makimoto, Appl. Phys. Lett. **85**, 4672 (2004).
[5] T. Ive, O. Brandt, H. Kostial, K. J. Friedland, L. Daweritz, and K. H. Ploog, Appl. Phys. Lett. **86**, 024106 (2005).
[6] E. Monroy, J. Zenneck, G. Cherkashinin, O. Ambacher, M. Hermann, M. Stutzmann, and M. Eickhoff, Appl. Phys. Lett. **88**, 071906 (2006).
[7] N. T. Son, M. Bickermann, and E. Janzen, Appl. Phys. Lett. **98**, 092104 (2011).
[8] N. T. Son, M. Bickermann, and E. Janzen, Phys. Status Solidi C **8**, 2167 (2011).
[9] C. H. Park and D. J. Chadi, Phys. Rev. B **55**, 12995 (1997).
[10] P. Boguslawski and J. Bernholc, Phys. Rev. B **93**, 9496 (1997).
[11] C. Stampfl and C. G. Van de Walle, Appl. Phys. Lett. **72**, 459 (1998).
[12] C. Stampfl and C. G. Van de Walle, Phys. Rev. B **65**, 155212 (2002).
[13] L. E. Ramos, J. Furthmüller, J. R. Leite, L. M. R. Scolfaro, and F. Bechstedt, Phys. Rev. B **68**, 085209 (2003).
[14] Y. Zhang, W. Liu, and H. Niu, Phys. Rev. B **77**, 035201 (2008).
[15] M. Hermann, F. Furtmayr, A. Bergmaier, G. Dollinger, M. Stutzmann, and M. Eickhoff, Appl. Phys. Lett. **86**, 192108 (2005).
[16] Y. Taniyasu, M. Kasu, and N. Kobayashi, Appl. Phys. Lett. **81**, 1255 (2002).
[17] P. Hohenberg and W. Kohn, Phys. Rev. **136**, B864 (1964).
[18] W. Kohn and L. J. Sham, Phys. Rev. **140**, A1133 (1965).
[19] C. Stampfl and C. G. Van de Walle, Phys. Rev. B **59**, 5521 (1999).
[20] M. Bockstedte, A. Kley, J. Neugebauer, and M. Scheffler, Comput. Phys. Commun. **107**, 187 (1997).
[21] C. G. Van de Walle and J. Neugebauer, J. Appl. Phys. **95**, 3851 (2004).
[22] S. B. Zhang and John E. Northrup, Phys. Rev. Lett. **67**, 2339 (1991).
[23] A. Rubio, J. L. Corkill, M. L. Cohen, E. L. Shirley, and S. G. Louie, Phys. Rev. B **48**, 11810 (1993).
[24] D. B. Laks, C. G. Van de Walle, G. F. Neumark, P. E. Blochl, and S. T. Pantelides, Phys. Rev. B **45**, 10965 (1992).
[25] Y. Li and D. W. Brenner, Phys. Rev. Lett. **92**, 075503 (2004).
[26] M. Hermann, F. Furtmayr, F. M. Morales, O. Ambacher, M. Stutzmann, and M. Eickhoff, J. Appl. Phys. **100**, 113531 (2006).
[27] S. B. Orlinskii, J. Schmidt, P. G. Baranov, M. Bickermann, B. M. Epelbaum, and A. Winnacker, Phys. Rev. Lett. **100**, 256404 (2008).
[28] V. Lebedev, F. M. Morales, H. Romanus, S. Krischok, G. Ecke, V. Cimalla, M. Himmerlich, T. Stauden, D. Cengher, and O. Ambacher, J. Appl. Phys. **98**, 093508 (2005).
[29] V. Serin, C. Colliex, R. Brydson, S. Matar, and F. Boucher, Phys. Rev. B **58**, 5106 (1998).
[30] R. Boger, M. Fiederle, L. Kirste, M. Maier, and J. Wagner, J. Phys. D: Appl. Phys. **39**, 4616 (2006).
[31] M. Pophristic, S. P. Guo, and B. Peres, Appl. Phys. Lett. **82**, 4289 (2003).
[32] D. C. Mueller, E. Alonso, and W. Fichtner, Phys. Rev. B **68**, 045208 (2003).
[33] M. Rummukainen, I. Makkonen, V. Ranki, M. J. Puska, K. Saarinen, and H.-J. L. Gossmann, Phys. Rev. Lett. **94**, 165501 (2005).